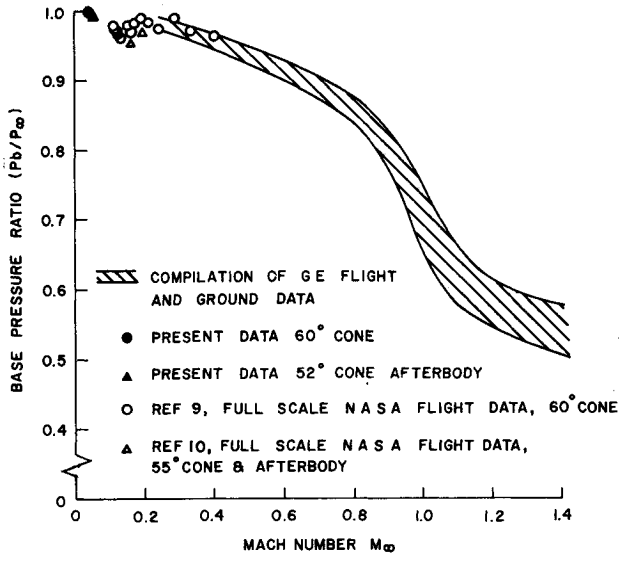

Fig. 10 Subsonic/transonic base pressure data.

angle of attack diverges (and hence the model is unstable) with increasing spin rate.

The second data source (the high speed movie camera) provided a significant amount of qualitative data. The 52° cone configuration appeared to be inherently more stable than the 60° configuration. That is, the 60° cone always diverged more than the 52° cone for the same spin rate. Actual photographic coverage of the 60° cone diverging is lacking, as the model was not tracked well due to the large degree of instability. In addition, the model divergence and hence trajectory perturbations were so great that the drop models tended to land outside the catcher net drop area. This resulted in a loss of a model at each drop, consequently repeat runs were available only until the 60° models were depleted. Two flat based 60° sharp edged models diverged and broke up upon impact and one 60° rounded edge model appeared to diverge even more than the sharp edge model.

The high speed movies show two basic trends which were repeatable: 1) Low-spin rate models tend to oscillate rapidly during the drop and tended to fall straight down and impact one to two feet from the reference back drop. 2) High-spin rate models tended not to oscillate, but rather trimmed up to a large angle of attack which produced a trajectory deflection resulting in an impact point five to seven feet from the reference back drop. Both were predicted by six-degree-of-freedom trajectory simulations for the drop test conditions. Thus the experimental drop test results verified the theoretical and numerical analyses showing a low speed blunt body instability. This phenomenon then places a restriction on the maximum spin rate allowable for some planetary missions.

Base pressure

The present base pressure drop test results[8] are compared in Fig. 10 with NASA Ames data.[9,10] The darkened symbols represent the present subscale drop test data while the open symbols represent full-scale flight results. Both sets of data are for similar configurations so that flight and ground data comparisons can be obtained directly by comparing similar open and closed symbols. Generally the data are in basic agreement and indicate that configuration differences apparently do not significantly alter the base pressure in subsonic flow. In addition the data demonstrate that base pressure varies from 0.95–0.99% of freestream pressure from $M_\infty \approx 0.4$ to 0.04. These results indicate that base pressure data from a planetary entry probe can be successfully utilized to derive the static freestream pressure profile of a planet during subsonic velocity conditions if the Mach number history of the probe is known.

References

[1] Seiff, A. and Reese, D., "Defining Mars' Atmosphere—A Goal for the Early Missions," *Astronautics & Aeronautics*, Vol. 3, No. 2, Feb. 1965, pp. 16–21.

[2] Buce, P. J. and Blyler, F., "Analysis of Venus '72 Probe Dynamics," TIS 67SD333, Nov. 1967, General Electric Co., King of Prussia, Pa.

[3] Murphy, C. H., "Free Flight Motion of Symmetric Missiles," Rept. 1216, July 1963, Ballistic Research Labs., Aberdeen Proving Ground, Md.

[4] Charters, A. C., "The Linearized Equations of Motion Underlying the Dynamic Stability of Aircraft, Spinning Projectiles and Symmetric Missiles," TN 3350, 1955, NACA.

[5] Shirley, D. L. and Misselhorn, J. E., "Instability of High-Drag Planetary Entry Vehicles at Subsonic Speeds," *Journal of Spacecraft and Rockets*, Vol. 5, No. 10, Oct. 1968, pp. 1165–1169.

[6] Coakley, T. J., "Dynamic Stability of Symmetric Spinning Missiles," *Journal of Spacecraft and Rockets*, Vol. 5, No. 10, Oct. 1968, pp. 1231–1232.

[7] Jaffe, P., "Terminal Dynamics of Atmospheric Entry Capsules," *AIAA Journal*, Vol. 7, No. 6, June 1969, pp. 1157–1158.

[8] Cassanto, J. M., "Subsonic Base Pressure Results on Typical Planetary Entry Configurations," *Journal of Spacecraft and Rockets*, Vol. 6, No. 5, May 1969, pp. 636–637.

[9] Sommer, S. and Yee, L., "An Experiment to Determine the Structure of a Planetary Atmosphere," AIAA Paper 68-1054, Philadelphia, Pa., 1968.

[10] Sommer, S., Boissevain, A., Yee, L., and Hedland, R., "The Structure of an Atmosphere from On-Board Measurements of Pressure, Temperature and Acceleration," TND-3933, 1967, NASA.

An Optimal, Analytic Solution to the Linear-Gravity, Constant-Thrust Trajectory Problem

DONALD J. JEZEWSKI*
NASA Manned Spacecraft Center, Houston, Texas

THE optimal two-point boundary value problem requires determination of the path, from an initial to a final boundary, which minimizes some performance index. If it is assumed that the transfer occurs in a vacuum and that the vehicle is propelled with a continuous constant thrust, then the optimal path is prescribed by the optimal thrust direction (identical to the direction of the primer), and the performance index to be minimized is the fuel consumption or time.

The primer vector and its derivative (the adjoint variables) are related to the position and velocity vectors (the state variables) by a set of linear differential equations, which are obtained by application of the calculus of variation to the differential equations of motion. This set of linear differential equations, which relate the adjoint variables to the state variables, must be integrated along with the state equations to obtain a closed-form solution of the optimal two-point boundary value problem.

In a previous study,[1] the gravitational acceleration vector was assumed to be a function of time only. The integrals of the adjoint equations for this assumption are trivial; the primer is a linear function of time. The state equations can be completely integrated to give six equations in terms of six unknowns. Thus, a closed-form solution is obtained that produces remarkably good results, with the chief limitation being that the thrusting arcs remain small.

Received August 8, 1970; revision received January 15, 1971.
* Aero Research Engineer. Member AIAA.

The present formulation is an extension of the study presented in Ref. 1. The gravitational acceleration vector is assumed to be not only a function of time but also a linear function of the radius vector. Hence, the previous study is a special case of the solution to be presented. The integrals of the adjoint equations are also trivial because the primer is represented by a homogeneous, second-order linear differential equation which is readily integrated. A solution of the state equations is obtained in terms of four integrals, two of which are tabularized and two of which are expandable in terms of known integrals. Therefore, an analytic solution for the position and velocity vectors is obtained in terms of the constants of integration of the adjoint and state equations.

Problem Description

Consider a vehicle in a rectangular Cartesian coordinate system which is disturbed by two external accelerations, gravity, and the acceleration caused by a thrusting force. The differential equations that describe the vehicle motion are

$$\dot{V} = g + l(T/m) \tag{1}$$

$$\dot{R} = V \tag{2}$$

$$\dot{m} = -T/V_E \tag{3}$$

where R, V, g, and l are the position, velocity, gravity acceleration, and thrust direction vectors, respectively. The gravity acceleration vector g is considered to be a function of position and time. If a constant thrust magnitude T and a constant mass flow rate $\dot{m}$ are assumed, a solution is sought (for a given set of boundary conditions) which will minimize the time interval $(t_1 - t_0)$. The effective exhaust velocity of the engine is represented by V_E.

The thrust direction vector is constrained by the relationship

$$l \cdot l = 1 \tag{4}$$

For the system of equations given in Eqs. (1–4) and for the assumptions which have been stated, the necessary conditions for an optimal solution (the adjoint equations) are

$$\dot{P} = -Q \tag{5}$$

$$\dot{Q} = -(P \cdot \nabla)g \tag{6}$$

$$(T/m)P = 2\epsilon l \tag{7}$$

where P, Q, and ϵ are time-varying Lagrange multipliers. (The multipliers P and Q are three-dimensional vectors, and ϵ is a scalar.) Lawden[2] has designated the vector P, the multiplier associated with the velocity vector, to be the primer. The analysis and solution to be presented will be expressed in terms of this vector and its components. From Eq. (7), note that the primer and thrust direction vectors are parallel if the undetermined multiplier ϵ is nonzero. The thrust-vector constraint expressed in terms of the primer is

$$P \cdot P = [2\epsilon/(T/m)]^2 \tag{8}$$

By elimination of ϵ from Eqs. (7) and (8), the relationship between the thrust direction vector and the primer vector becomes

$$l = \pm P/|P| \tag{9}$$

Lawden used the Weierstrass condition to show that the plus sign is correct for this problem and that the directions of the primer and thrust vectors are identical.

Problem Solution

In the derivation of the necessary conditions for the optimal solution, the gravity acceleration vector has been assumed to be a function of position and time. Furthermore, the degree of success that can be achieved when an optimal analytic solution is being obtained is highly dependent on the form of this gravity acceleration vector. For example, in a previous study,[1] ∇g was assumed to be zero; therefore, the vector g was required to be a function of time only. For this assumption, the primer is a linear function of time, and the equations of motion can be integrated completely (without further approximation) to give 1) six equations in terms of the boundary conditions on the state, 2) the six constants of the vector P, and 3) the solution interval $(t_1 - t_0)$. Not all the constants of the primer are independent since they appear in the equations of motion as a ratio [Eq. (9)]. The closed-form solution obtained with this assumption produced remarkably good results, with the main limitation being that the thrusting arcs remain small, less than approximately $\pi/6$ rad. If restriction of the gravity acceleration vector to be a function of time produces reasonably good results, then perhaps it is better to choose this vector to vary both as a function of time and as a linear function of the position vector. Let the gravity acceleration vector be represented by

$$g = G(t) - \omega^2 R \tag{10}$$

where G is a vector function of time, and ω is a scalar constant. By use of this assumption in Eq. (6), the vector multiplier $\dot{Q}$ is of the form

$$\dot{Q} = \omega^2 P \tag{11}$$

and the primer, determined by use of Eqs. (5) and (11), is represented by the following homogeneous, second-order, linear differential equation:

$$\ddot{P} = -\omega^2 P \tag{12}$$

The solution for P and Q is represented by

$$P = A \sin\omega t + B \cos\omega t \tag{13a}$$

$$Q = -\omega(A \cos\omega t - B \sin\omega t) \tag{13b}$$

where A and B are three-dimensional vector constants of integration. Thus, for a linear gravitational field and a constant thrust, the optimal vector acceleration is expressed by the equation

$$\ddot{R} + \omega^2 R = G + (a_0/\mu)P/|P| \tag{14}$$

where Eqs. (2, 9, and 10) have been used. The quantity μ is the normalized mass ratio

$$\mu = m/m_0 = 1 + t\,\dot{\mu} \tag{15}$$

and the constant a_0 is the initial thrust-to-mass ratio T/m_0. Equation (14) is an ordinary, second-order, linear differential equation. In physical problems, Eq. (14) represents the motion of a harmonic oscillator without damping but with a forcing function represented by the right-hand side of the equation. The solution of Eq. (14) is obtained by the combination of a solution for the reduced or complementary equation with a particular solution. The reduced equation

$$\ddot{R} + \omega^2 R = 0 \tag{16}$$

has as a solution

$$R = C \sin\omega t + D \cos\omega t \tag{17}$$

where C and D are constants of integration, each a three-dimensional vector. A general method used to determine a particular solution is the method of variation of parameters. This method of solution considers the constants C and D to be variables which satisfy the following differential equations:

$$\dot{C} \sin\omega t + \dot{D} \cos\omega t = 0 \tag{18a}$$

$$\omega(\dot{C}\cos\omega t - \dot{D}\sin\omega t) = G + (a_0/\mu)P/|P| \quad (18b)$$

The complete solution for Eq. (14) is obtained by solving Eqs. (18a) and (18b) for C and D (where new constants of integration C_1 and D_1 will occur) and by using these solutions in Eq. (17). The solutions for C and D are

$$C = C_1 + (1/\omega)(I_1 + a_0 I_2) \quad (19a)$$

$$D = D_1 - (1/\omega)(I_3 + a_0 I_4) \quad (19b)$$

where

$$I_1 = \int G\cos\omega t dt \qquad I_2 = \int \frac{P}{|P|}\frac{\cos\omega t dt}{\mu} \quad (20a)$$

$$I_3 = \int G\sin\omega t dt \qquad I_4 = \int \frac{P}{|P|}\frac{\sin\omega t dt}{\mu} \quad (20b)$$

and the general solution for the position vector is expressed as shown in Eq. (17). The integrals defined in Eq. (20) are evaluated in the Appendix. The velocity vector is obtained by differentiation of Eq. (17) to obtain

$$V = \omega(C\cos\omega t - D\sin\omega t) + \dot{C}\sin\omega t + \dot{D}\cos\omega t \quad (21)$$

It may be readily verified that the last two terms in Eq. (21) add to zero and that the position and velocity vectors may therefore be written in the simplified matrix equation

$$\begin{bmatrix} R \\ V \end{bmatrix} = \begin{bmatrix} \sin\omega t & \cos\omega t \\ \omega\cos\omega t & -\omega\sin\omega t \end{bmatrix}\begin{bmatrix} C \\ D \end{bmatrix} \quad (22)$$

The constants C_1 and D_1 are determined by evaluation of Eqs. (19) and (22) at some convenient reference time. The solution for these constants at a time $t_0 = 0$ is

$$C_1 = V_0/\omega - 1/\omega(J_1 + a_0 J_2) \quad (23a)$$

$$D_1 = R_0 + 1/\omega(J_3 + a_0 J_4) \quad (23b)$$

where $R_0 = R(t_0)$, $V_0 = V(t_0)$, and

$$J_i = I_i(t_0) \qquad i = 1, 2, \ldots, 4 \quad (24)$$

Numerical Example

Since atmospheric forces have not been considered in the solution, an example problem was chosen for an orbital transfer where this force was either absent or negligibly small. The example problem chosen was a constant thrust burn from a circular earth orbit at an altitude of 53.96 km with the primer P chosen to be a unit vector along the Y axis, and Q, a unit vector at an angle of $\pi/4$ rad to the X and Y axis.

Figure 1 lists the initial conditions (R,V,P,Q) [the vector $G(t)$ equal to zero, the gravitational constant equal to unity] and the vehicle characteristics for this problem. The figure illustrates the error as a function of W_1/W_0, the ratio of the burnout weight to initial weight. The error E was computed by taking the logarithm to the base 10 of the difference in the magnitudes of the vectors obtained by solving Eqs. (13) and (22) and the solution obtained by integrating the nonlinear differential equations. The two solutions used the same initial conditions. A fourth-order Runge-Kutta integration package with a constant step size of one-hundredth of the time interval was used for the integration of the nonlinear equations. Note for example that an error of -4 corresponds to four significant digits of accuracy, which for this problem represents approximately a position error of 0.65 km and a velocity error of 0.75 m/sec.

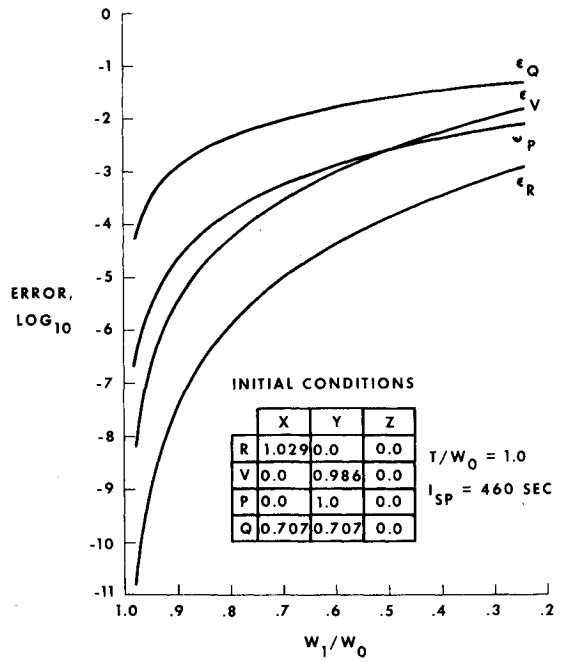

Fig. 1 Error as a function of W_1/W_0.

Appendix A: Evaluatian of Integrals

To evaluate $I_1, \ldots, I_4$ of Eqs. (20a) and (20b) (where the vector $P = A\sin\omega t + B\cos\omega t$; $\mu = 1 + \dot{\mu}t$; $G = G(t)$; and A, B, and $\dot{\mu}$ are constants), let the function $G(t)$ be represented by a polynomial in time of the form

$$G = \sum_{n=0}^{N} \Lambda_n t^n \quad (A1)$$

where Λ_n is a three-dimensional vector, the components of which are constants. Then, the solution for the integral I_1 is given by the following recursive equation:

$$I_1 = \sum_{n=0}^{N} \Lambda_n \left(\frac{t^n\sin\omega t}{\omega} - \frac{n}{\omega}\int t^{n-1}\sin\omega t dt\right) \quad (A2)$$

The solution for I_3 is the same, except $\sin\omega t$ is replaced by $(-\cos\omega t)$. The integrals I_2 and I_4 are more complicated and require some manipulation for their evaluation. By use of the definition of μ and P, the integral I_2 is found to be

$$I_2 = \int \frac{(A\sin\omega t + B\cos\omega t)dt}{(1 + \dot{\mu}t)(\alpha\tan^2\omega t + \gamma\tan\omega t + \beta)^{1/2}} \quad (A3)$$

where $\alpha = A\cdot A$, $\beta = B\cdot B$, and $\gamma = 2A\cdot B$. An apparent change of variable is

$$z = \tan\omega t \quad (A4)$$

The integral I_2 expressed in terms of z is

$$I_2 = \frac{1}{\omega}\int \frac{(Az + B)dz}{(1 + z^2)^{3/2}(1 + b_0\tan^{-1}z)Z^{1/2}} \quad (A5)$$

where $b_0 = \dot{\mu}/\omega$, and $Z = \alpha z^2 + \gamma z + \beta$.

The integral I_2 has no known solution; however, it is possible to expand a portion of the integrand in a series form such that the interval of integration is well contained in the interval of convergence. For the interval $(-\pi/4 < \omega t < \pi/4)$, the terms $(1 + z^2)^{-3/2}$ and $(1 + b_0\tan^{-1}z)$ may be expanded as

$$(1 + z^2)^{-3/2} = a_1 + a_2 z^2 + a_3 z^4 + \ldots a_n z^{2n-2}$$

$$(1 + b_0\tan^{-1}z) = b_1 + b_2 z + b_3 z^3 + \ldots b_n z^{2n-3} \quad (A6)$$

where

$$a_1 = b_1 = 1, \quad a_{n+1} = (-1)^n \prod_{i=1}^{n} \left(\frac{2i+1}{2i}\right)$$

$$b_{n+1} = \frac{(-1)^{n+1} b_0}{2n-1}, \quad n = 1, 2, 3 \ldots$$

The quotient of these two series[3] is thus of the form

$$\frac{(1+z^2)^{-3/2}}{(1+b_0 \tan^{-1} z)} = c_1 + c_2 z + c_3 z^2 + \ldots c_n z^{n-1} \quad \text{(A7)}$$

where $c_1 = 1$, and for n odd

$$c_{n+1} = -\sum_{i=1}^{(n+1)/2} b_{i+1} c_{n-2(i-1)}$$

and for n even

$$c_{n+1} = a_{\frac{n+2}{2}} - \sum_{i=1}^{n/2} b_{i+1} c_{n-2(i-1)}$$

By using Eq. (A7) in Eq. (A5), the integral I_2 may be written as

$$I_2 = \frac{1}{\omega} \int \frac{(c_1 + c_2 z + c_3 z^2 + \ldots c_n z^{n-1})(Az + B)dz}{Z^{1/2}} \quad \text{(A8)}$$

The integral I_2 may be termwise integrated for the bounded interval $(-\pi/4 < \omega t < \pi/4)$.

The solution for the integral I_2 may be written as

$$I_2 = (1/\omega)[c_1 B K_1 + (c_1 A + c_2 B) K_2 + (c_2 A + c_3 B) K_3 + \ldots (c_{n-1} A + c_n B) K_n] \quad \text{(A9)}$$

where the K's are evaluated[4] at $n = 1, 2, 3, \ldots$ from

$$K_1 = \int \frac{dz}{Z^{1/2}} = \frac{\sinh^{-1}}{\alpha^{1/2}} \left(\frac{2\alpha z + \gamma}{q^{1/2}}\right) \quad \text{(A10)}$$

and $q = 4\alpha\beta - \gamma^2$

$$K_2 = \int \frac{z dz}{Z^{1/2}} = \left(\frac{Z^{1/2}}{\alpha} - \frac{\gamma}{2\alpha} K_1\right) \quad \text{(A11)}$$

The $(n+1)$th term

$$K_{n+1} = \left[z^{n-1} Z^{1/2} - \frac{(2n-1)\gamma K_n}{2} - (n-1)\beta K_{n-1}\right] \Big/ n\alpha \quad n = 2, 3, 4 \ldots \quad \text{(A12)}$$

By using Eq. (A4), the remaining integral I_4 is written as

$$I_4 = \frac{1}{\omega} \int \frac{(Az + B) z dz}{(1+z^2)^{3/2}(1 + b_0 \tan^{-1} z) Z^{1/2}} \quad \text{(A13)}$$

By use of a procedure similar to that used with integral I_2, the solution for integral I_4 is as shown in

$$I_4 = (1/\omega)[c_1 B K_2 + (c_1 A + c_2 B) K_3 + (c_2 A + c_3 B) K_4 + \ldots (c_{n-1} A + c_n B) K_{n+1}] \quad \text{(A14)}$$

where $K_2, K_3, \ldots, K_{n+1}$ are evaluated in Eqs. (A11) and (A12).

References

[1] Jezewski, D. J. and Stoolz, J. M., "A Closed-Form Solution for Minimum-Fuel, Constant-Thrust Trajectories," *AIAA Journal*, Vol. 8, No. 7, July 1970, pp. 1229–1234.

[2] Lawden, D. F., *Optimal Trajectories for Space Navigation*, Butterworths, London, 1963.

[3] Fulks, W., *Advanced Calculus, An Introduction to Analysis*, Wiley, New York, 1961, Chap. 16.

[4] Peirce, B. O., *A Short Table of Integrals*, 4th ed., revised by R. M. Foster, Ginn, Boston, Mass., 1956.

Analysis of Sprays from Rocket Engine Injectors

W. H. NURICK*

Rocketdyne/North American Rockwell Corporation, Canoga Park, Calif.

OVER the last 15 years, the importance of obtaining uniformity of liquid propellant "mixing" to obtain high combustion efficiency in rocket engines has been shown both analytically and experimentally.[1–6] While these studies have contributed to an understanding of the influence of propellant distribution on combustion efficiency, they did not define the interrelationship between the quality of the over-all propellant mixing and the resulting mixing-limited combustion efficiency. An analytical relationship of this type is needed in preliminary design of rocket engine injectors to compare analytically the effect of spray quality on combustion efficiency for various propellant combinations. It should be pointed out that atomization is also an important parameter limiting the performance obtained in most rocket engines. This paper, however, considers only mixing effects on combustion efficiency.

Mixing and combustion occur in three principal zones: 1) in the prereaction zone the propellants are atomized into sprays and mixed; 2) vaporization and combustion are initiated; and 3) as combustion proceeds, the resulting gas accelerates the flow down the chamber in a stream tube manner. While some transverse mixing occurs in the combustion zones, experimental data show that the combustion performance calculated from the mass and mixture ratio (MR) distribution at the end of the prereaction zone agree quite well with that actually obtained.[7]

This Note describes an analytical model defining the relationship between the propellant spray mixing quality determined using cold-flow measurements (see Ref. 7 for details) and combustion performance. Experimental verification of the results predicted from cold-flow analysis is also described. Comparisons are then made of the effect of mixing uniformity on the c^* mixing limited performance for various propellant combinations.

Mixing Quality

Following Rupe[1] we define the mixing quality as the sum of the mass-weighted deviations in mixture ratio from the injected mixture ratio. Rupe considers the cumulative distribution plot for a nonuniform mixture and a monodisperse mixture as shown in Fig. 1. (Monodisperse mixture is here defined as a bipropellant mixture having completely constant mixture ratio in both space and time.) In Fig. 1, $r \equiv MR/(1 + MR)$ at any point in the mixture, and R is the value of r corresponding to the injected mixture ratio. With these definitions, the mass having $r < R$ is to the left and the mass having $r > R$ is to the right of the monodisperse line ($r \equiv R$).

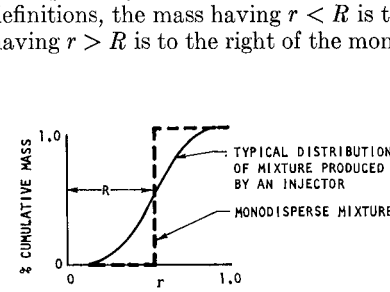

Fig. 1 Normalized mass and mixture ratio distribution plot.

Received December 14, 1970; revision received February 19, 1971. The data presented in this paper was obtained under AFRPL Contract AF04(611)-67-C-0081 and NASA Contract 3-11199.

* Member of Technical Staff. Member AIAA.